EBBR-SIRS Net Radiation Difference: An Evaluation

D.R. Cook and D.J. Holdridge
Argonne National Laboratory
Argonne, Illinois

Abstract

Accurate radiation measurements are a crucial goal of the ARM Program. Therefore, the large observed differences in net radiation between the EBBR and SIRS instrument systems are a source of concern. EBBR net radiation is, on average, greater than SIRS net radiation by typically 50 W m^{-2} during clear days and 40 W m^{-2} during clear nights. The source of the difference is mostly in the infrared, not the shortwave. The effective sky temperature sensed by the two instrument systems is a significant factor, this being very obvious at night under different cloud cover conditions. For clear sky at night the differences are large; for a continuous low cloud cover or for fog conditions the differences are small. The net radiation measurements of the two instruments are compared with a side-by-side comparison outside at NREL, comparisons at ARM SGP ARCF sites, and IR blackbody calibrations performed at ANL. A recent recognition of a -12 W m^{-2} bias in the NREL calibration procedure does not help to explain the difference. Explanations for the differences in IR measurements are given.

Introduction

The goal of this study was to characterize causes of the difference in longwave net radiation (Net IR) measured by the SIRS Eppley pyrgeometers (PIR) and the EBBR REBS Q*7.1 net radiometer. The Net IR differences range from nearly 0 W m^{-2} (Figure 1a) during heavy cloud cover or fog, to 25 W m^{-2} (Figure 1b) on a night with thin clouds, to 50 W m^{-2} (Figure 1c) on a cloudless night during winter, (Figure 1c). The SIRS Net IR is normally smaller than the EBBR Net IR and on many cloudless nights the SIRS Net IR is twice the magnitude of the EBBR Net IR. The difference between the two systems is also present during daytime and therefore the EBBR Net IR is typically greater than the SIRS Net IR during daytime with an offset similar to the nighttime difference. Radiometer calibration problems, apparently, sometimes result in deviations from these generalities. A PIR calibration bias of 12 W m^{-2} was recently discovered by the SIRS mentor, but if all PIRs are similarly affected, the SIRS Net IR may not be affected by this bias.

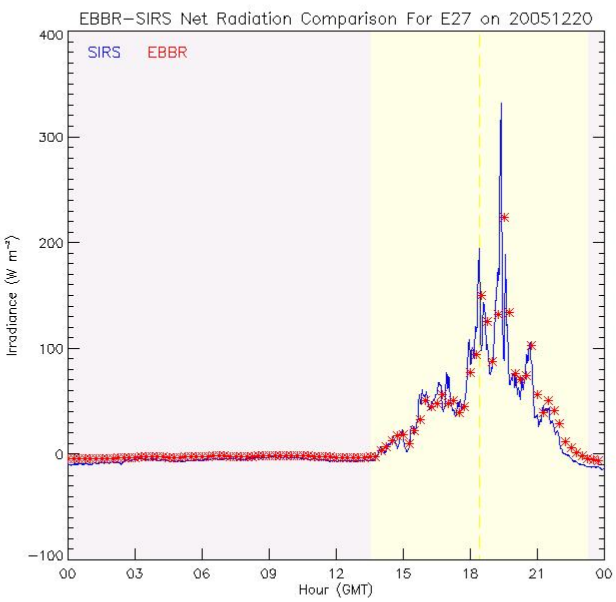

Figure 1a.

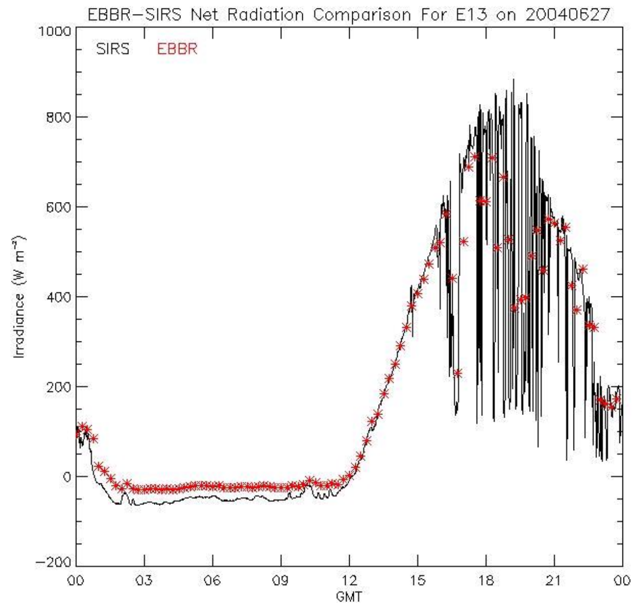

Figure 1b.

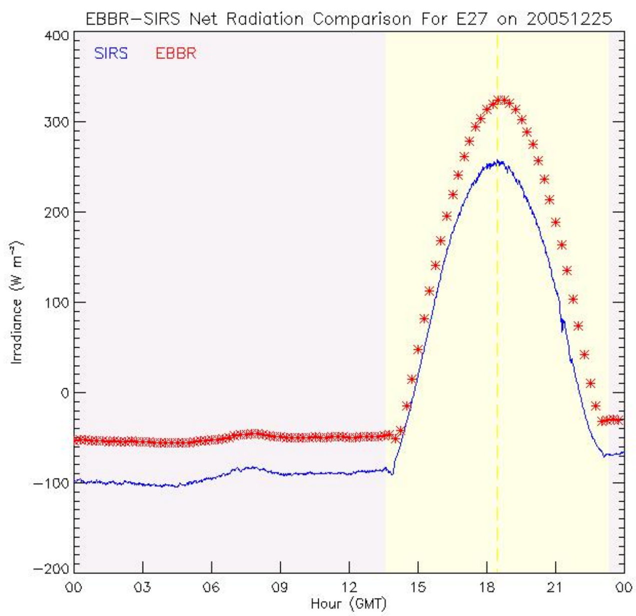

Figure 1c.

PIR, Q*7.1 Physical Differences

There are significant physical differences between the PIR and Q*7.1 sensors that must be recognized. The importance of these differences in their ability to accurately measure Net IR is not well known. The PIR sensing surface is mounted in a heavy metal case and covered by a tellurium/zinc selenide coated silicon dome. The silicon dome blocks all shortwave radiation and the coating on the inside of the dome allows transmittance in the 3.5 to 50 um range, according to Eppley PIR specifications. However, the long wavelength specification may be overstated. The transmittance characteristics of tellurium (3.85 to 31 um) and zinc selenide (0.58 to 22 um) are well documented in journal articles, and would therefore appear to restrict the PIR to a measurement range of 3.85 to 22 um. Perhaps the combination of the two substances extends this range. It is not an important point since the range of terrestrial longwave is approximately 3.5 to 22 um. The PIR is adjusted for measured dome and case temperatures, with these adjustments often being of similar magnitude to the infrared measurement itself. Therefore, careful calibration is needed to make the adjustments properly.

The Q*7.1 net radiometer has optical black sensing surfaces that are enclosed in hard plastic and covered with virgin polyethylene domes. The two sensing surfaces are placed back-to-back, thereby ensuring a common base temperature reference for the thermopiles encased below the sensing surfaces. REBS claims a transmittance range of 0.25 to 60 um for the Q*7.1. However, the shortwave end of the range may be overspecified, as journal articles indicate that the transmittance capability of polyethylene is 0.32 um to about 100 um. At any rate, the transmission range allows the passage of UVA through terrestrial IR wavelengths. UV light produces photoproducts on the outside surface (at least) of the polyethylene domes, resulting in a significant decrease in UVA transmittance and a slight decrease in visible transmittance (due to “clouding” of the polyethylene) after a few months of exposure to the Sun, as well as a strong decrease in transmittance at 5 um and some decrease at 8-12 um and 2.8-3.2 um. Furthermore, transmittance in polyethylene is weak at the wavelengths of strongest IR transmission by water vapor, possibly introducing a systematic water vapor dependent error into the Q*7.1 IR measurement.

Outdoor Comparisons

A REBS Q*7.1, Eppley PIRs and PSPs, Kipp and Zonen (K&P) CNR-1 net radiometer, and a number of other radiometers were compared outdoors for several months at the NREL radiometer test facility to attempt to detect net radiation measurement differences in a somewhat controlled setting. Figures 2a and 2b show a comparison of net radiation from the Q*7.1, Eppley, and K&P sensors for cloudy and clear conditions, respectively. On the cloudy night of late 18 Aug 2004, the Q*7.1 and the K&P were different by less than 1 m^{-2} but the Eppley net radiation was 10 W m^{-2} lower than the Q*7.1. On the clear night of late 29 Aug 2004 the K&P was 24 W m^{-2} lower than the Q*7.1 and the Eppley was 33 W m^{-2} lower than the Q*7.1. The difference between the Eppley and K&P was about 10 W m^{-2} no matter what the sky condition, which may suggest a regular offset in one or both; their calibration slopes are very similar. The difference between the Eppley and Q*7.1 for clear and cloudy conditions was 24 W m^{-2}, which is less than what is often observed at the SGP ACRF. These measurements suggest that the Q*7.1 may have a systematic Net IR calibration slope error for low sky temperatures.

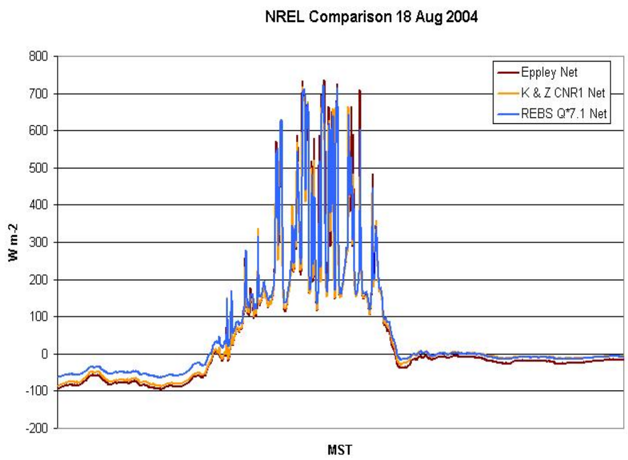

Figure 2a.

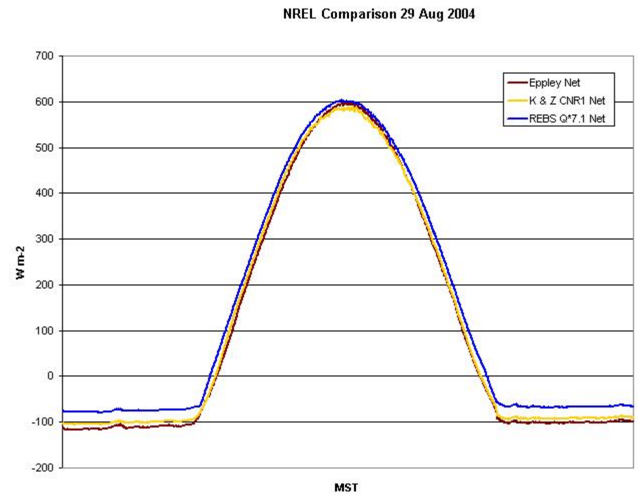

Figure 2b.

Figure 3a provides an example of the change in Net IR that accompanies a change in sky condition, and therefore a change in sky and surface temperature. Figure 3b shows a small change in surface temperature (5.5°C) in response to the change in sky temperature (83°C in Figure 3c) as a clear sky with temperature 185°K gave way to a cloud deck with temperature 268°K over the SGP Central Facility early on 20 January 2004. The Q*7.1 Net IR measurement changed 34 W m^{-2} and the PIR Net IR measurement changed 57 W m^{-2} for an 88.5°C change in surface-sky temperature difference. The difference between the PIR and Q*7.1 for clear versus cloudy conditions was 23 W m^{-2}, nearly the same as for the similar conditions that occurred during the NREL comparison mentioned above.

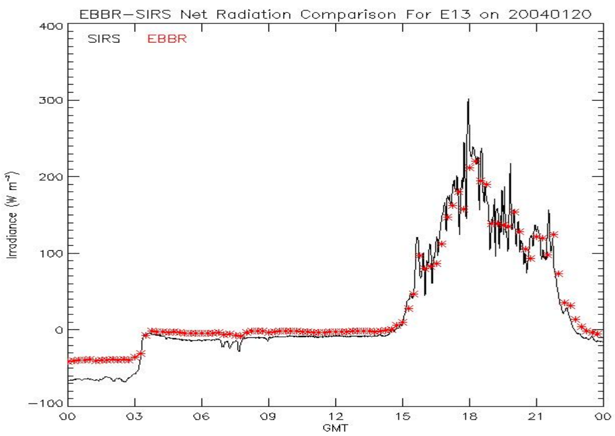

Figure 3a.

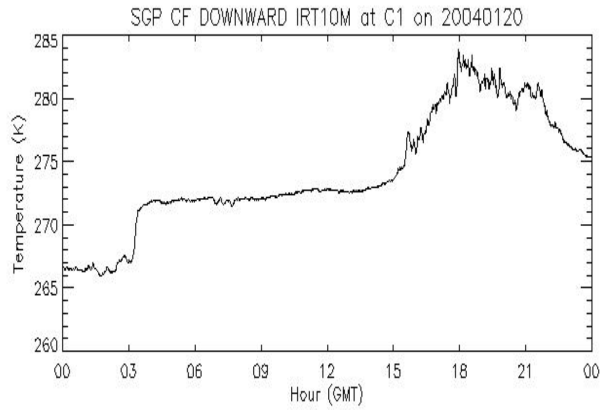

Figure 3b.

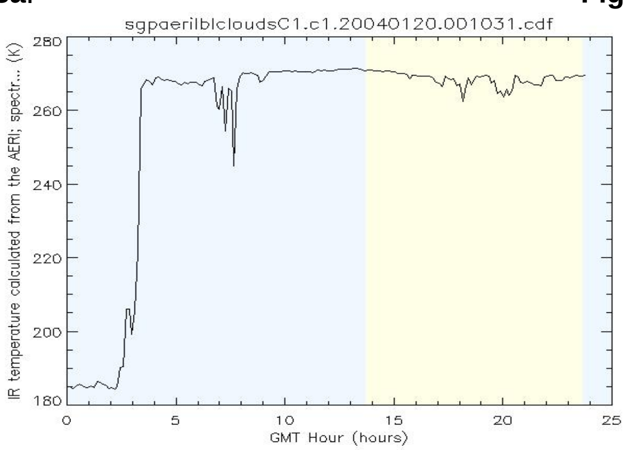

Figure 3c.

Radiometric and meteorological data from the SGP ACRF Central Facility was averaged for middle of the night hours (0300-1000 GMT) for each day of 2004 to provide information on meteorological and radiometric effects on Net IR measurements. The EBBR provided meteorological data, the AERI provided sky temperature, and the 10 m IRT provided ground surface temperature. Nighttime net radiation is smaller in mid-summer than during mid-winter, a reflection primarily of warmer surface temperatures in summer. Sky temperatures are somewhat greater in summer than in winter. Meteorological measurements of ambient temperature, relative humidity, and wind speed did not have a significant affect on the Q*7.1 or PIR measurements. Figure 4a compares the PIR Net IR with the Q*7.1 Net IR for the range of difference in sky and ground temperatures encountered during 2004, and Figure 4b shows the sky temperature measured by the AERI and the ground temperature measured by the 10 m IRT. The slopes of the two scatter plots in Figure 4a are different and reveal a consistent calibration difference throughout the range of measurements. Both the Q*7.1 and PIR Net IR also exhibit a small negative offset for no difference in sky and ground temperature. The PIR data is also plotted individually versus ground and sky temperature in Figures 4c and 4d. Note the minimal scatter in ground temperature in comparison with sky temperature, as expected.

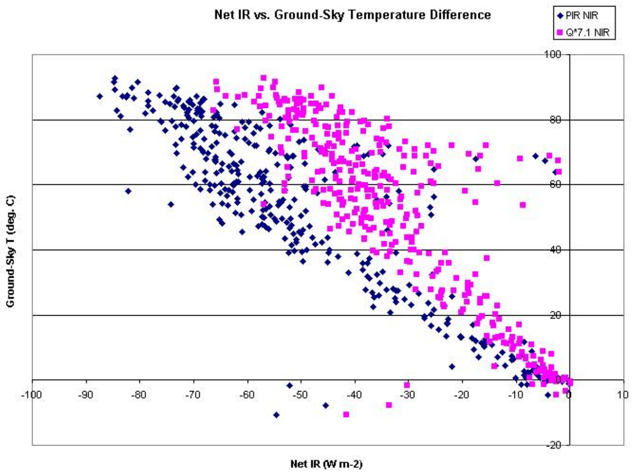

Figure 4a.

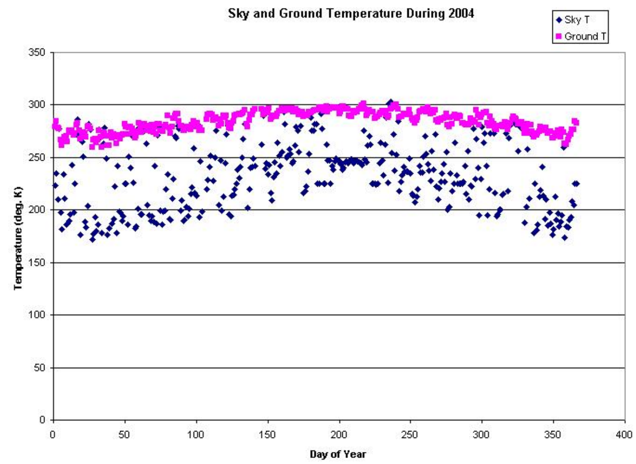

Figure 4b.

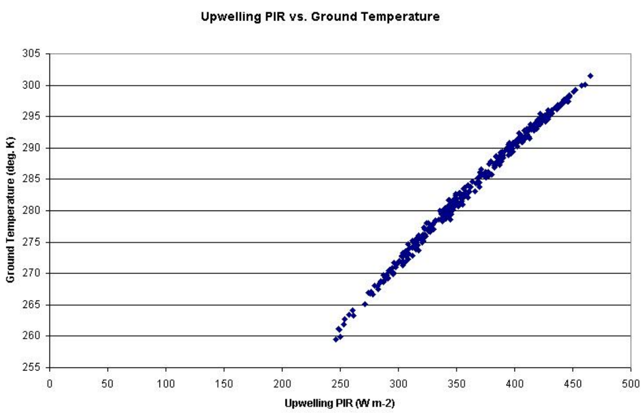

Figure 4c.

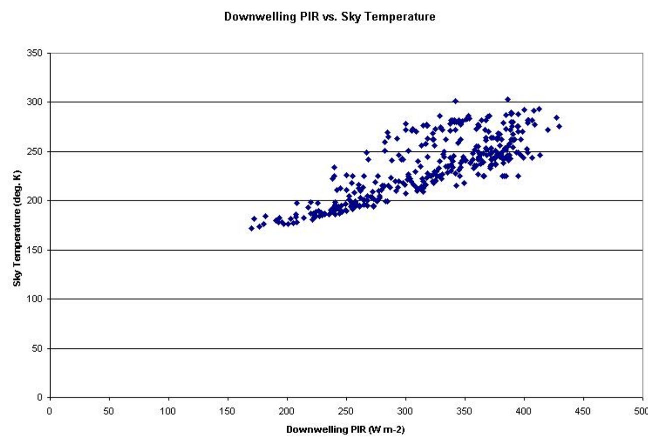

Figure 4d.

IR Calibrations

Beyond the obvious, and dramatic, physical differences of the PIR and Q*7.1, there is also the significant difficulty of performing precise IR calibrations on those sensors. IR calibrations are normally performed using blackbody temperature sources in well controlled laboratory conditions. The SIRS mentor has stated that "Pyrgeometer blackbody calibration differences are greatest during clear sky conditions (high levels of net radiation) and least during cloudy sky periods (low levels of net radiation)." The same is likely true for the REBS Q*7.1 net radiometer and points up the possibly deleterious impact of not being able to perform IR calibrations at the wide range of sky and terrestrial temperatures (-100°C to 30°C) experienced at the ARM SGP ACRF. This calibration inadequacy may partially explain the range of SIRS Net IR difference between the SGP extended facilities.

REBS calibrates the Q*7.1 for IR at 21° and 30°C to obtain a nighttime calibration slope. This small range of temperatures seems inadequate for the wide range of sky and ground temperatures encountered naturally, especially considering that the PIR is calibrated down to a much lower -35°C. It has been stated that -35°C is assumed to simulate clear sky conditions, for purposes of PIR IR calibrations. However, the AERI clearly shows that -35°C actually reflects cloudy conditions, even during summer, and does not reflect clear sky conditions, which exhibit temperatures of -100°C in winter to -60°C in summer.

Two PIRs and a Q*7.1 (the same one used in the NREL outdoor comparison) were compared against Mikron blackbody references. IR temperatures used in the comparison ranged from -20°C to 100°C. Comparisons were performed for the Q*7.1 and PIRs for three ambient temperatures: approximately 6°C, 26°C, and 32°C. The comparisons also allowed us to see the behavior of the PIR and Q*7.1 for differences in ambient temperature. The Q*7.1 was compared to the blackbodies and then flipped over to see if there was a systematic bias in the calibration of one side. Other than very small 1 to 3 W m^{-2} offsets at zero Net IR, no systematic difference was seen for the two orientations of the Q*7.1 or between the two PIRs checked.

No significant difference was seen between using the downwelling PIR ventilated and unventilated. However, the Q*7.1 showed a significantly larger output when not ventilated. Ventilation of the Q*7.1 domes, particularly for higher blackbody temperatures, must greatly reduce the polyethylene dome temperature, keeping it nearer ambient temperature. Keeping the domes near ambient temperature probably suppresses the response to temperature extremes.

Figure 5 shows the blackbody comparison results for one of the PIRs; the results for the other PIR were so similar that they are not included in the figure, for clarity. The PIRs were compared with the blackbody standards using the Eppley four coefficient technique, which does not properly account for case temperature. Therefore, significant offsets are seen between the three ambient temperature curves. This points up one of the concerns of using the Eppley four coefficient calibration in the place of the NREL calibration technique.

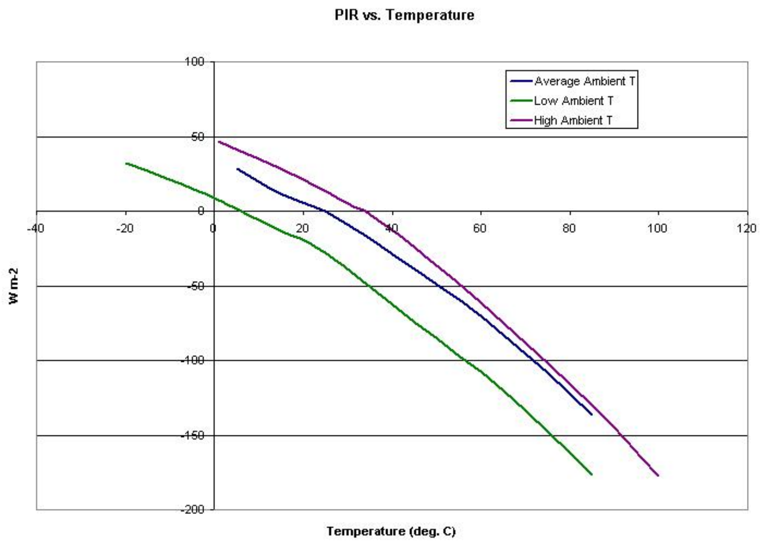

Figure 5.

Sky temperature similar to what occurs naturally (left of the Figure 5 graph origin) could only be obtained for a very limited range (to -20°C) with the equipment that was available, and therefore the comparisons do not improve on low temperature calibrations performed by ARM. The plotted curves are clearly not linear in any temperature range. The data plotted to the right of the origin simulates natural ground temperatures (up to about 40°C) and well beyond. Although ground temperatures above 40°C are not natural at SGP, the greater concern is the significant change in curve slope at higher temperatures. If the PIR also experiences a significant change in slope for very low temperatures (which the sensor is not calibrated for), IR may be somewhat under-measured for these conditions.

Figure 6 shows the blackbody comparison results for the Q*7.1. The red curve shows the result for the Q*7.1 flipped, with output sign reversed, just to show that the behavior is the same as for the normal, upright orientation. A small output offset of about 2-3 W m^{-2} is seen for the 26°C case. A significant difference in slope and offset is seen between the results at 26°C and the results at 6°C and 32°C. The 6°C offset is largest (-18 W m^{-2}, as opposed to 5.7 W m^{-2} at 32°C), indicating scaling with ambient temperature. This offset is not accounted for in the Q*7.1 calibration. Only the points of the red and dark blue curves near zero represent the conditions used in the Q*7.1 IR calibration; these yield a slope of 0.46 W m^{-2}°C^{-1}. The slope for low sky temperature or high ground temperature (the latter does not occur at SGP) is about 0.90 W m-2°C^{-1}. The curves in Figure 6 form an "s" shape, with a larger slope for extreme sky, ground temperature differences. The difference in slope between extreme temperature difference and the slope near zero (which represents the conditions under which the Q*7.1 is calibrated) is approximately a factor of 2, which is the typical difference in nighttime IR measurement of the PIRs and the Q*7.1. It seems likely then that the Q*7.1 is under-measuring IR during both daytime and nighttime because of the temperature range limitation in the manufacturer's IR calibration, and this explains most of the difference seen in net radiation between the PIRs and the Q*7.1.

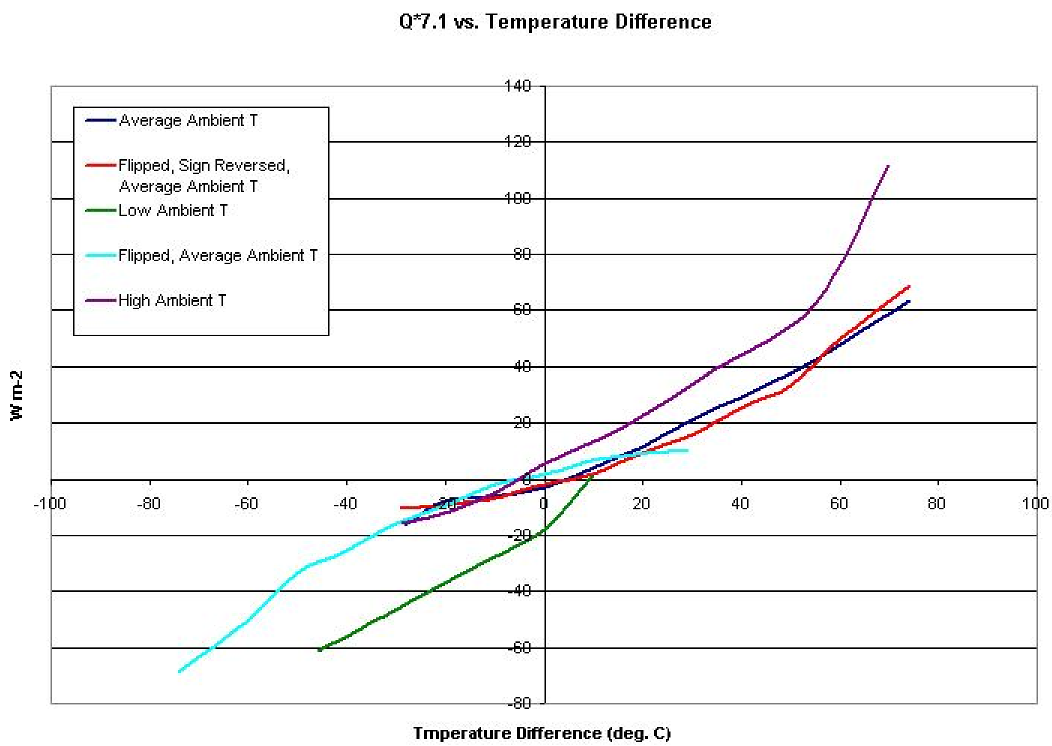

Figure 6.

Summary

Neither the PIR nor the Q*7.1 are adequately calibrated in the IR for cloudy to clear sky temperature conditions in any season. Furthermore, the range of calibration temperatures used for the Q*7.1 IR calibration is particularly limited. The PIR exhibits very large offsets for different case temperatures when the Eppley four coefficient calibration equation is used and it also exhibits a significant change in calibration slope at high temperatures, which may be replicated at low temperatures. The Q*7.1 exhibits an "s" shape curvature in its calibration, the consequence of which is that it appears to underestimate IR by a factor of two under most sky conditions. Improvements in the IR cold temperature calibration range of both sensors are warranted; without such improvements, the quality of cloudy and clear sky IR and net radiation measurements is questionable.

Tutorial: EBBR and SIRS

Energy balance Bowen ratio (EBBR): The Energy Balance Bowen Ratio (EBBR) system uses the gradient approach to produce 30 min estimates of the vertical fluxes of sensible and latent heat. Flux estimates are calculated from observations of net broadband radiation, soil surface heat flux, and the vertical gradients of temperature and vapor pressure. Other measurements include wind speed, wind direction, near surface soil temperature, near surface soil moisture, barometric pressure, and relative humidity. Data collected by the EBBR are also used to calculate bulk aerodynamic fluxes with the Bulk Aerodynamic Technique (BA) EBBR value-added product (VAP), to replace sunrise and sunset spikes in the flux data. A unique aspect of the system is the automatic exchange mechanism (AEM), which helps to reduce errors from instrument offset drift by switching the gradient instruments from upper to lower positions or vice versa every 15 minutes. Accuracy of the flux measurements is approximately +/- 10%, with a tendency to overestimate latent heat flux. There are 14 EBBR systems installed at SGP ACRF extended facilities and 1 proposed for the Darwin site at the TWP ACRF.

Solar and Infrared Radiation Station (SIRS): The Solar Infrared Radiation Station (SIRS) provides continuous measurements of broadband shortwave (solar) and longwave (atmospheric or infrared) irradiances for downwelling and upwelling components. One minute average data are collected from a network of stations to help determine the total energy exchange within the SGP ACRF. Each SIRS consists of sensors to measure various wavelengths of solar and terrestrial radiation, including direct beam normal shortwave, diffuse horizontal shortwave, global horizontal shortwave, shortwave reflected from the surface, longwave emitted from the sky, and longwave emitted by the surface. A solar tracker is used to keep some of these sensors pointed directly at the Sun. There are 22 SIRS installed at SGP ACRF extended facilities and the same suite of sensors is installed in the GNDRAD/SKYRAD systems at each of the TWP ACRF and NSA ACRF facilities.